

# An X-ray Tour of Massive Star-forming Regions with Chandra

By LEISA K. TOWNSLEY<sup>1</sup>

<sup>1</sup>Department of Astronomy and Astrophysics, Pennsylvania State University, 525 Davey Laboratory, University Park, PA 16802, USA

The Chandra X-ray Observatory is providing fascinating new views of massive star-forming regions, revealing all stages in the life cycles of massive stars and their effects on their surroundings. I present a *Chandra* tour of some of the most famous of these regions: M17, NGC 3576, W3, Tr14 in Carina, and 30 Doradus. *Chandra* highlights the physical processes that characterize the lives of these clusters, from the ionizing sources of ultracompact HII regions (W3) to superbubbles so large that they shape our views of galaxies (30 Dor). X-ray observations usually reveal hundreds of pre-main sequence (lower-mass) stars accompanying the OB stars that power these great HII region complexes, although in one case (W3 North) this population is mysteriously absent. The most massive stars themselves are often anomalously hard X-ray emitters; this may be a new indicator of close binarity. These complexes are sometimes suffused by soft diffuse X-rays (M17, NGC 3576), signatures of multi-million-degree plasmas created by fast O-star winds. In older regions we see the X-ray remains of the deaths of massive stars that stayed close to their birthplaces (Tr14, 30 Dor), exploding as cavity supernovae within the superbubbles that these clusters created.

---

## 1. Revealing the Life Cycle of a Massive Stellar Cluster

High-resolution X-ray images from the Chandra X-ray Observatory and XMM-Newton elucidate all stages in the life cycles of massive stars – from ultracompact HII (UCHII) regions to supernova remnants – and the effects that those massive stars have on their surroundings. X-ray studies of massive star-forming regions (MSFRs) thus give insight into the massive stars themselves, the accompanying lower-mass cluster population, new generations of stars that may be triggered by the massive cluster, interactions of massive star winds with themselves and with the surrounding neutral medium, and the fate of massive stars that die as cavity supernovae inside the wind-blown bubbles they created.

In the era of *Spitzer* and excellent ground-based near-infrared (IR) data, why are X-ray studies of MSFRs important? *Chandra* routinely penetrates  $A_V > 100$  mag of extinction with little confusion or contamination, revealing young stellar populations in a manner that is unbiased by the presence of inner disks around these stars. These vast pre-main sequence (pre-MS) populations are easily seen by *Chandra* and the  $17' \times 17'$  imaging array of its Advanced CCD Imaging Spectrometer (ACIS-I); a typical ACIS-I observation of a nearby ( $D < 3$  kpc) MSFR, lasting 40–100 ksec, finds 500–1500 young stars, tracing the initial mass function (IMF) down to  $\sim 1M_\odot$ . These observations can increase the number of known cluster members by as much as a factor of 50 in poorly-studied regions (e.g. NGC 6357, J. Wang et al. 2006).

In the first 7 months of 2006, at least 18 refereed papers on X-ray observations of MSFRs (using *Chandra* or *XMM*) were published or submitted. These include studies of 30 Doradus (Townesley et al. 2006a,b), NGC 6334 (Ezoe et al. 2006),  $\sigma$  Orionis (Franciosini et al. 2006), Westerlund 1 (Skinner et al. 2006; Munro et al. 2006), RCW 38 (Wolk et al. 2006), Cepheus B/OB3b (Getman et al. 2006), NGC 6357 (J. Wang et al. 2006), M17 (Broos et al. 2006), NGC 2362 (Delgado et al. 2006), NGC 2264 (Flaccomio et al. 2006; Rebull et al. 2006), Trumpler 16 in Carina (Sanchawala et al. 2006), NGC 6231

(Sana et al. 2006), the Orion Nebula Cluster (Stassun et al. 2006), the Arches and Quintuplet clusters (Q. Wang et al. 2006), and W49A (Tsujiimoto et al. 2006). Early *Chandra* and *XMM* studies were summarized in Townsley et al. (2003); more recent work is described in Feigelson et al. (2006). Other MSFRs currently under study at Penn State include RCW 49 (Townsley et al. 2004), NGC 7538 (Tsujiimoto et al. 2005), W51A (Townsley et al. 2004, 2005), and the Rosette Nebula (Wang et al. 2006, in preparation).

This contribution begins with recent X-ray results on the young MSFRs M17 and NGC 3576, two regions at different evolutionary stages but with notably similar outflows of hot, X-ray-emitting gas. Next I introduce a new ACIS mosaic of the Westerhout 3 complex, showing how triggered star formation in the same molecular cloud can result in very different stellar clusters. Then I address the rich and complicated point source and diffuse X-ray emission seen towards Trumpler 14 in Carina. Finally I provide a first look at a new *Chandra* observation of 30 Doradus obtained in early 2006.

## 2. M17, The Omega Nebula: An X-ray Champagne Flow

The Omega Nebula (M17) is the second-brightest HII region in the sky (after the Orion Nebula). Its OB cluster NGC 6618 probably has well over 5000 members, extending up to masses  $M \sim 70 + 70M_{\odot}$  (spectral type O4V+O4V) in its central binary. It is situated at the edge of one of the Galaxy's most massive and dense molecular cloud cores, M17SW, at a distance of 1.6 kpc (Nielbock et al. 2001). It is a blister HII region viewed nearly edge-on, on the periphery of a giant molecular cloud (GMC) containing an UCHII region with UV-excited water masers and active star formation. The ionization front of the HII region encounters the GMC along two photodissociation regions, called the northern and southern bars. With an age of  $< 1$  Myr (Hanson et al. 1997) and no evolved stars, M17 is one of the few bright MSFRs that has sufficient stellar wind power to produce an X-ray outflow and yet is unlikely to have hosted any supernovae.

We observed M17's central cluster NGC 6618 with *Chandra*/ACIS-I for 40 ksec in March 2002. The extensive soft diffuse emission seen in M17 is rare; it was described by Townsley et al. (2003) and is shown in Figure 1. The 877 point sources detected in this observation are described, catalogued, and compared to IR data by Broos et al. (2006). Fewer than 10% of these point sources (in M17 and in the other Galactic MSFRs described here) are unrelated to the MSFR (foreground stars and background AGN, J. Wang et al. 2006). *Chandra* has a point spread function (PSF) that is sub-arcsecond on-axis, but degrades radially to become many arcseconds wide at the field edge. This effect is apparent in Figure 1 and in other ACIS images shown in this paper.

Figure 1 (right) shows the  $5.8\mu\text{m}$  GLIMPSE image of M17 from the Spitzer Space Telescope's Infrared Array Camera (IRAC). The early *Chandra* and *Spitzer* images in Figure 1 show dramatic and complex interacting components of hot and cold material. On the western side of the cluster, the parsec-scale thermalized O-star winds shock the parental GMC, triggering new massive star formation to the southwest. To the east, the winds escape the confinement of the blister HII region producing the brightest known X-ray champagne flow, heating and chemically enriching the ISM (Townsley et al. 2003).

*Chandra*'s strongly-varying PSF and the ACIS-I camera's large field of view also make it difficult to convey the sub-arcsecond imaging quality in full-field smoothed images. Figure 2 (left) shows the central  $\sim 25''$  of the M17 ACIS image, binned to  $0.25''$  pixels. NGC 6618's central binary is separated by  $\sim 2''$  and is clearly resolved. These are the brightest X-ray sources in the field (Broos et al. 2006). Figure 2 (right) shows their spectra and model fits. Each source was fit using *XSPEC* (Arnaud 1996) with a two-temperature *apex* thermal plasma model (R. Smith et al. 2001), including absorption.

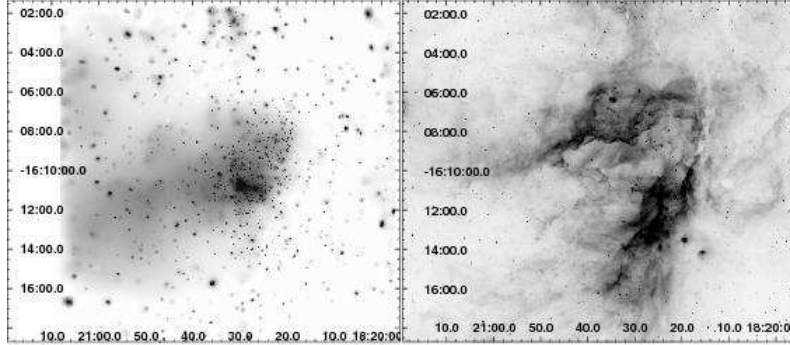


FIGURE 1. **Left:** Smoothed 0.5–2 keV ACIS-I image of M17 ( $\sim 8$  pc across), highlighting the soft diffuse X-ray emission. Here and throughout this paper, coordinates are J2000 RA and Dec. **Right:** *Spitzer*/IRAC 5.8 $\mu$ m image of the same M17 field, part of the GLIMPSE survey and provided by the GLIMPSE team. This pair of images highlights both the rich stellar population revealed through X-ray/IR comparison studies and the complementarity of the two Great Observatories for mapping diffuse emission in the region.

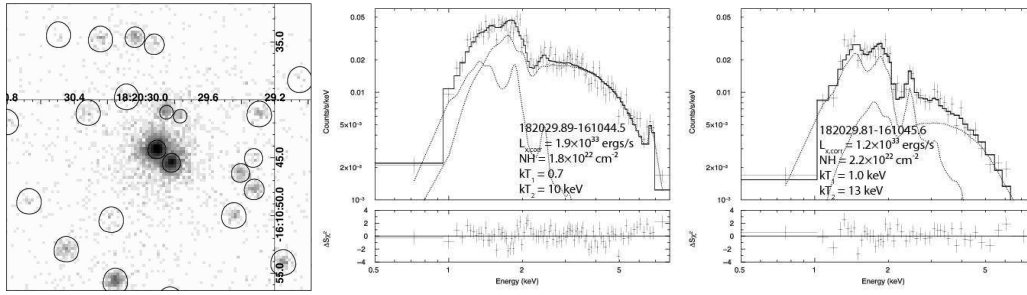


FIGURE 2. **Left:** High-resolution ACIS image of the central region of NGC 6618 in M17, highlighting the bright O4+O4 binary. The nearly-circular polygons mark the photometric and spectral extraction regions for each source. **Center and Right:** ACIS spectra of the two O4 stars. For each source, the top panel shows the event data as a histogram, each component of the model (convolved with the instrumental response) as dotted lines, and the composite model as a solid line. The lower panel shows the fit residuals.

The soft plasma components in these O4 stars are of similar strength and are typical of O stars; they are thought to be due to microshocks in the powerful stellar winds. Both of these sources, however, show very hard thermal plasmas as well; the brighter O4 star’s spectrum is dominated by this hard component. A reasonable explanation for this hard emission is that it comes from colliding winds in an as-yet-unrecognized close binary system. Since both O4 stars exhibit this hard emission, it is possible that the O4+O4 binary actually consists of no fewer than 4 massive components.

### 3. The Giant HII Region NGC 3576: An M17 Analog?

NGC 3576 is a Galactic giant HII region, located at a distance of 2.8 kpc (de Pree et al. 1999). It contains several known O and early B stars but these are not sufficient to account for the Ly $\alpha$  ionizing photons inferred from radio data (Figuerêdo et al. 2002). An embedded massive IR star cluster is located at the edge of its GMC (Persi et al. 1994). It contains at least 51 stars earlier than A0, most with large IR excesses. It likely includes as yet unrecognized O stars that would account for the number of Ly $\alpha$  photons.

A radio study of NGC 3576 (de Pree et al. 1999) revealed a large north-south velocity

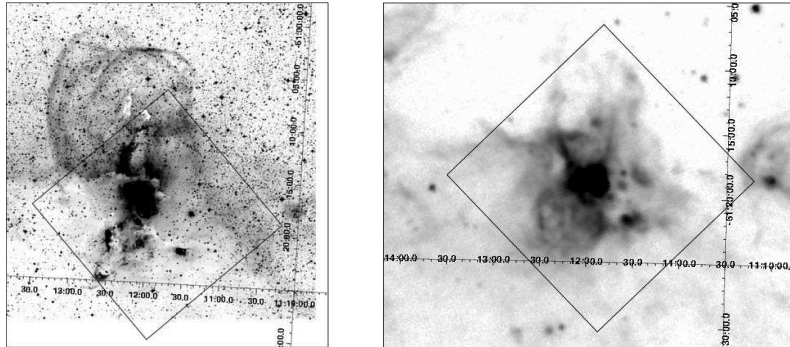


FIGURE 3. NGC 3576 images. **Left:** Digital Sky Survey red band. **Right:** *MSX*  $8\mu\text{m}$ . The black squares show the size and approximate roll angle of the ACIS-I array.

gradient in the ionized gas of the nebula, indicating a large-scale ionized outflow. This flow may contribute to the large loops and filaments seen in visual data (Figure 3, left). The  $8\mu\text{m}$  *MSX* image (Figure 3, right) is complementary to the visual data, revealing heavy obscuration in the southern half of the field and what appears to be a bipolar bubble likely blown by the massive stars in NGC 3576’s central cluster. This bubble appears closed to the south, where it encounters the dense GMC, but open to the north, in the same direction as the large visual loops.

In July 2005 we obtained a 60-ksec ACIS observation of NGC 3576, to see if a soft X-ray bubble suggested by the *ROSAT* data was indicating that NGC 3576 possessed an X-ray outflow similar to that seen in M17. The ACIS aimpoint was directed at the strong infrared source IRS 1, at the core of the embedded young stellar cluster, to search for embedded protostars and the stellar sources responsible for ionizing NGC 3576, as well as to resolve the brightest flaring pre-MS stars. Our ACIS field here is similar to that for M17: only part of the bubble seen by *ROSAT* is captured. It was important to keep the aimpoint on IRS 1, though, to study the embedded population and the IR cluster, which hold the key to understanding the source of the *ROSAT* bubble.

Figure 4 (left) shows that this observation indeed reveals the massive stellar engine powering NGC 3576, shredding the molecular cloud from which it formed. Many sources not known even from mid-IR studies (e.g. Maercker et al. 2006) are seen in X-rays. The brightest of these is a hard, deeply-embedded source  $\sim 20''$  south of IRS1. This and other new X-ray sources may be the long-sought embedded massive stars providing the extra ionization for NGC 3576.

Much of the X-ray bubble seen by *ROSAT* is resolved by *Chandra* into a wide array of point sources distributed across the field. Diffuse X-rays remain, however, near the top of the ACIS field and in a more concentrated patch southeast of the central cluster. Comparing the smoothed ACIS image (Figure 4, right) to the visual and mid-IR data in Figure 3, it appears that the northern visual loops outline (at least in part) soft diffuse X-ray emission in and beyond the northern, more open lobe of the bipolar bubble. Throughout the field the diffuse X-ray emission is complementary to the mid-IR emission, suggesting either that warm dust has displaced the hot X-ray gas or that this material is shadowing the X-rays, absorbing and obscuring any soft X-ray emission that may lie behind it. The southern lobe is also traced by soft diffuse X-ray gas; the lack of shadowing here implies that this part of the wind-blown bubble lies on the near side of the GMC. There are clear relationships between NGC 3576’s X-ray plasma, velocity and temperature gradients measured in the radio, the impressive visual loops, and the

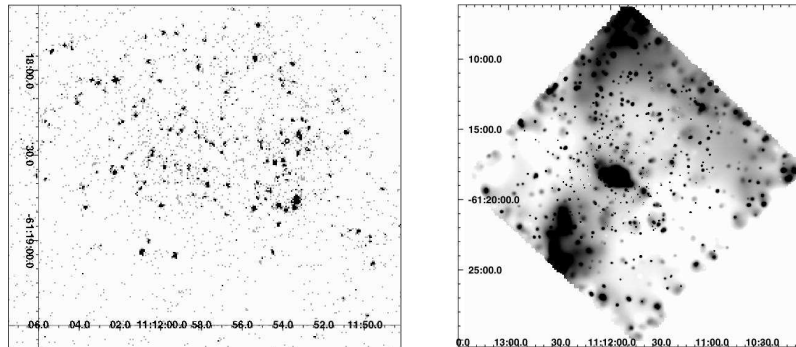


FIGURE 4. NGC 3576 ACIS-I data. **Left:** The central cluster. The approximate position of IRS1 is marked with a small black circle. **Right:** Full-band (0.5–8 keV) smoothed image.

mid-IR bipolar bubble. Spectral analysis of this diffuse X-ray emission is ongoing and should give some insight into the energetics of this important complex.

*Chandra* has revealed that NGC 3576 and M17 are two examples of the same phenomenon, although NGC 3576’s cluster is younger and more deeply embedded in its natal cloud, leading to the more complex spatial morphology in its soft diffuse X-ray emission. It appears that hot, flowing X-ray gas from OB winds may be a common component of young blister HII regions, strongly affecting their morphology and dynamics.

#### 4. W3: Ionizing Sources Revealed and a Missing Cluster

W3 is a large, nearby ( $D = 2.0$  kpc, Hachisuka et al. 2006) MSFR in the Perseus Arm of the Milky Way. The W3 complex contains one of the most massive molecular clouds in the outer Galaxy (Heyer & Terebey 1998), massive embedded protostars (Megeath et al. 2005), near- and mid-IR sources (Kraemer et al. 2003), masers, and outflows. It is unique in containing all morphological classes of HII region, from hypercompact to diffuse, 0.01 to 1 pc in diameter, with ages  $10^3$ – $10^6$  yrs (Tieftrunk et al. 1997).

Many authors have argued that star formation in W3 is being induced by the expansion of the adjacent W4 superbubble, which is sweeping up molecular gas into a high-density layer, within which stars are forming. Oey et al. (2005) revised this scenario, proposing that the young (3–5 Myr) OB cluster IC 1795, triggered to form by W4, is blowing its own second-generation superbubble at the molecular cloud interface, triggering in turn the W3 complex of massive star formation. W3 is an ideal testbed for understanding recent, ongoing, and triggered star formation; X-ray sources there are all at the same distance yet exist in a range of dynamical settings, providing a series of controlled environments in which to study the violent interactions of massive stars with their natal cloud.

With many observations throughout 2005, used ACIS-I to image the three major star-forming complexes, W3 North, W3 Main, and W3(OH), amassing  $\sim 80$  ksec on each field. A mosaic of these observations is shown in Figure 5. ACIS resolves the OB stars powering the HII regions, embedded massive stars and protostellar objects, and the pre-MS population, yielding  $> 1300$  X-ray sources in the three  $\sim 80$  ksec pointings.

W3 North is a well-developed parsec-scale HII region powered by the O6V star GSC 04050-02567 that may be isolated, with no lower-mass accompanying population (Carpenter et al. 2000). The HII region is so bright in the near-IR due to nebular emission that it is difficult to perform an IR search for an underlying cluster. *Chandra* detects the O6 star; it is a modest, soft X-ray emitter, typical of single O stars. However Figure 5 clearly reveals that W3 North is not an Orion-like field; no cluster of young X-ray-emitting pre-MS stars

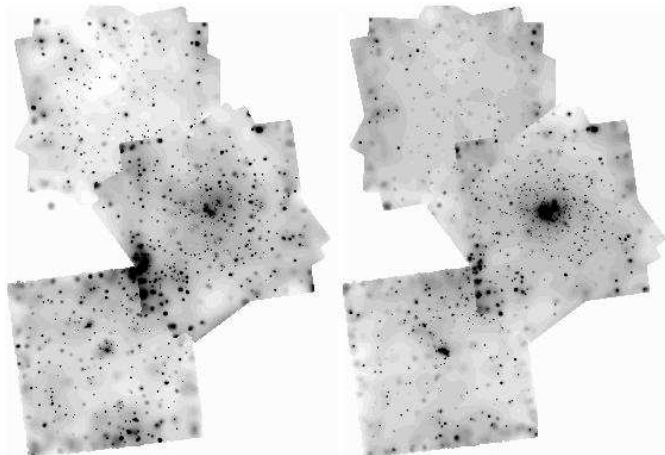


FIGURE 5. **Left:** Smoothed soft-band (0.5–2 keV) ACIS-I mosaic of W3 North (top), W3 Main (middle), and W3(OH) (bottom). The slightly older OB cluster IC 1795 is partially imaged between W3 Main and W3(OH). **Right:** Hard-band (2–8 keV) mosaic of the same W3 regions.

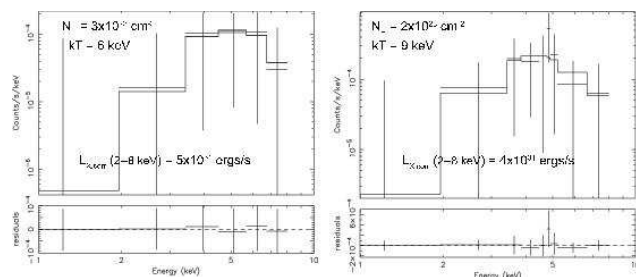


FIGURE 6. ACIS spectra of embedded W3 protostars. **Left:** W3 Main IRS5. **Right:** W3(OH).

is seen. This may indicate that the region has an anomalous IMF, that this O6 star is a young example of a massive star that formed in isolation (de Wit et al. 2005), or that the O6 star is a runaway from either IC 1795 or W3 Main that has somehow managed to create a large and complex HII region at the edge of W3’s high-density layer. In any case, this is an unusual situation that merits more detailed study.

W3 Main harbors the strongest CO peak in W3 and IR clusters with over 200 stars (Carpenter et al. 2000). An early 40-ksec ACIS-I observation showed possible extended emission spatially coincident with the HII regions; over 100 of the 236 ACIS sources detected in this original dataset are near the W3 core (Hofner et al. 2002). We added another 40 ksec to this original observation; in the composite image, it is clear that W3 Main is the dominant star-forming center of W3, with an extensive population of young stars nearly filling the  $17' \times 17'$  ACIS-I field of view. The full extent of W3 Main was not clear from earlier IR studies. Of the  $> 1300$  sources in the W3 ACIS mosaic, over half of them are captured in the W3 Main pointing.

W3(OH) contains the B0.5 star IRAS 02232+6138 surrounded by a cluster of more than 200 stars (Carpenter et al. 2000), an UCHII region ( $2''$  in diameter), OH and H<sub>2</sub>O masers, outflows, IR sources, and strong CO indicating massive embedded protostars. ACIS detects a point source associated with the W3(OH) UCHII region and resolves the string of known IR stellar clusters northeast of W3(OH) that may indicate a broader region of ongoing star formation (Tieftrunk et al. 1997).

Figure 6 shows the ACIS spectra of two interesting embedded sources in the W3 complex: IRS5 in W3 Main and the X-ray source in W3(OH), presumably the source of ionization for the UCHII region. IRS5 is thought to be a multiple system of perhaps five proto-OB stars (Megeath et al. 2005). We don't resolve the components with ACIS, but we do find a very hard spectrum for the X-ray source coincident with IRS5, again consistent with colliding-wind binary emission, although this hard emission could be coming from a cluster wind generated by the combined effects of the winds from all of these massive protostars (Cantó et al. 2000). The W3(OH) source is also extremely hard. Due to the high obscuration toward these sources, we have no information on any soft X-ray emission that they might be generating. The luminosities that we note in Figure 6 are corrected for this absorption, but are only given for the hard (2–8 keV) X-ray band.

## 5. Trumpler 14: Swarms of Stars and Misplaced Hot Gas

The Carina complex is part of the Sagittarius-Carina spiral arm, at a distance of  $\sim 2.3$  kpc (N. Smith 2006b). It is a remarkably rich star-forming region, containing 8 open clusters with at least 66 O stars, several Wolf-Rayet (WR) stars, and the luminous blue variable Eta Carinae (N. Smith 2006a). The combined Carina OB clusters Tr16, Tr14, and Cr228 contain the nearest rich concentration of early O stars; their ionizing flux and winds may be fueling a young bipolar superbubble (N. Smith et al. 2000). High ISM velocities throughout the complex (Walborn et al. 2002b) and the presence of evolved stars may imply that a supernova might already have occurred in this region, although no well-defined remnant has ever been seen.

Tr14 is an extremely rich, young ( $\sim 1$  My), compact OB cluster near the center of the Carina complex, containing at least 30 O and early B stars (Vázquez et al. 1996). The radio HII region Carina I is situated just west of Tr14, at the edge of the GMC and near a strong CO peak. It is ionized by Tr14 and is carving out a cavity in the molecular cloud which now contains *IRAS* sources, high-mass protostars, their associated UCHII regions, and ionization fronts (Brooks et al. 2001). Although star formation has ceased in the Keyhole region of Carina due to the harsh environment created by the massive stars there, the proximity of Tr14 to the GMC has triggered a new generation of star formation in Carina I (Rathborne et al. 2002).

In September 2004 we obtained a 57-ksec ACIS-I observation of Tr14 (Figure 7). The aimpoint of this observation is the central star in the cluster, HD 93129AB, a very early-type (O2I–O3.5V) binary (Walborn et al. 2002a), with the two components separated by  $\sim 3''$ . Our ACIS-I observation reveals  $\sim 1600$  X-ray point sources in the Tr14 region, suffused by bright, soft diffuse emission. Since the Tr16 and Tr14 clusters overlap, some sources toward the east and southeast are most likely Tr16 members; a few sources in the northeast corner of our field may be members of the nearby Tr15 cluster. The soft diffuse emission pervading the eastern half of our field is sharply cut off to the west by the GMC. The density of X-ray point sources also falls sharply to the west, due in part to reduced sensitivity because of higher extinction and in part because star formation is just now being triggered in that region, as described above.

Figure 8 (left) shows the crowded central region of Tr14 in X-rays, with the source extraction regions drawn. The brightest source near field center is HD93129A; it is clearly resolved from HD93129B (seen slightly to the southeast) and from another, fainter star just to its south (west of HD93129B). The ACIS spectra of these early O stars are shown in Figure 8 (right panel). Although these two stars are of similar early spectral type, they show remarkably different X-ray spectra. While both exhibit the expected soft thermal plasma with  $kT \sim 0.5$  keV, HD93129A also requires a second, harder thermal

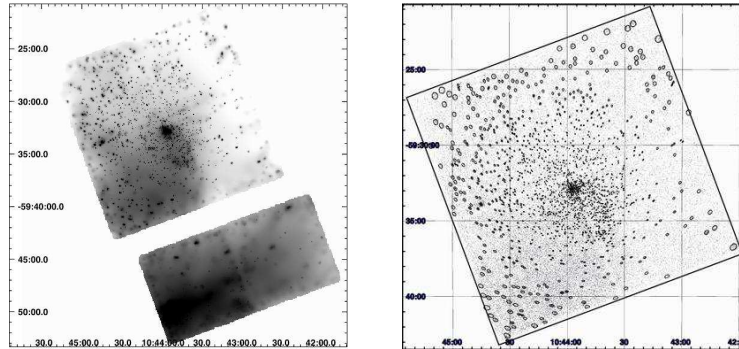


FIGURE 7. ACIS images of Tr14 in Carina. **Left:** Full-field, full-band smoothed image. **Right:** The ACIS-I image (binned by  $2''$ ), showing  $\sim 1600$  point source extraction regions.

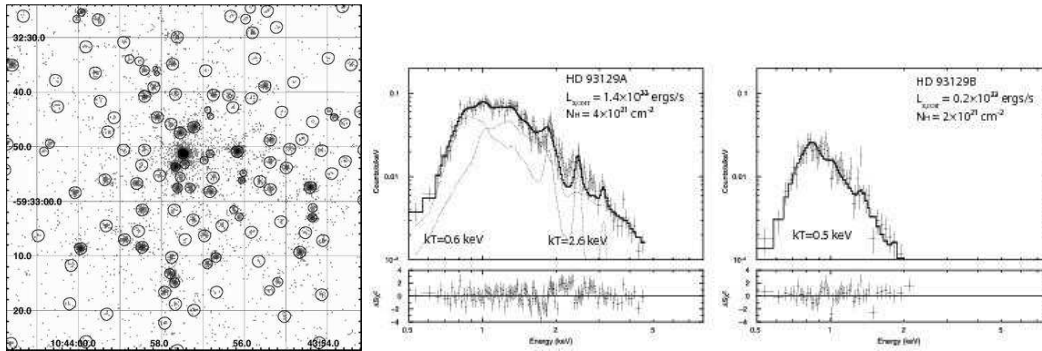


FIGURE 8. **Left:** The central part of the ACIS-I observation of Tr14 with extraction regions marked. **Center:** ACIS spectrum of the resolved massive binary at the aimpoint of the Tr14 observation, HD93129A (O2If) and **Right:** HD93129B (O3V).

component and is 7 times brighter in X-rays than HD93129B. We find similar results for other O stars in the field: while the O3V star HD93128 is soft ( $kT = 0.3$  keV) and faint (absorption-corrected luminosity  $L_{X,\text{CORR}} = 0.1 \times 10^{33}$  ergs/s), the O3V star HD93250 is the brightest source in the ACIS field, with  $L_{X,\text{CORR}} = 2.1 \times 10^{33}$  ergs/s and requiring both soft ( $kT = 0.6$  keV) and hard ( $kT = 3.3$  keV) thermal plasma components. As for other sources described above, this leads us to speculate that HD93129A and HD93250 could be colliding-wind binaries; alternatively the hard components of their spectra are soft enough that they could be magnetically active early O stars, similar to  $\theta^1$  Ori C (Gagné et al. 2005). In contrast, HD93129B and HD93128 are likely more “normal” O stars without these phenomena.

The soft diffuse emission seen in this ACIS observation of Tr14 (Figure 9, left) is also remarkable. On the ACIS-I array, this diffuse emission is brightest in the southeast quadrant, in the region between Tr14 and Tr16. Surprisingly, it is not centered on the Tr14 cluster. The apparent surface brightness of this emission may be affected by gradients in the absorbing column across the field. We serendipitously imaged very bright diffuse emission in the off-axis ACIS-S CCDs that were also operational for this observation. This emission is far from the known massive stars in the Carina complex. Although its apparent surface brightness is much higher than the diffuse emission seen on the ACIS-I array, it is intrinsically fainter; we see it as brighter because it suffers no measurable absorption. This may indicate that it lies in front of the Tr14 cluster, perhaps partially filling the lower lobe of the Carina superbubble seen in the mid-IR.

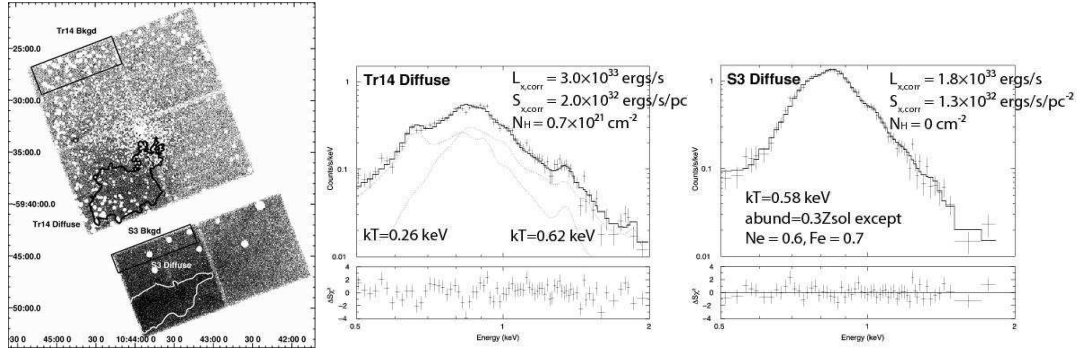


FIGURE 9. Diffuse emission in Tr14. **Left:** Image showing point sources removed, with diffuse extraction regions marked. **Center and Right:** Spectra of the two diffuse regions.

While both regions of diffuse emission exhibit soft spectra (Figure 9), they require quite different model fits. The emission in the southeast quadrant of the I array requires a two-temperature fit ( $kT = 0.3$  keV and  $kT = 0.6$  keV), some absorption, and typical low abundances of  $Z = 0.3Z_{\odot}$ . The S array emission requires just a single thermal component with  $kT = 0.6$  keV, but no absorbing column is seen and a good fit is only obtained by increasing the abundances of Ne and Fe, possibly indicating a supernova origin for this emission. Earlier X-ray data suggested that the Carina complex is pervaded by diffuse X-ray emission not concentrated on the star clusters. This detailed view from *Chandra* now shows that the diffuse emission is spatially and spectrally complex and, while it may be due in part to massive star winds, one or more cavity supernovae probably also contribute to its complexity. More high-resolution observations of the Carina MSFR are necessary to untangle this complicated mix of pointlike and diffuse X-ray sources.

## 6. 30 Doradus: Live Fast, Die Young, Blow Some Bubbles

30 Doradus in the Large Magellanic Cloud is the most luminous Giant Extragalactic HII Region and “starburst cluster” in the Local Group. At the center of 30 Dor is the “super star cluster” R136, with dozens of 1-2 Myr-old  $> 50 M_{\odot}$  O and Wolf-Rayet stars (Massey & Hunter 1998). 30 Dor’s superbubbles are well-known bright X-ray sources, where multiple cavity supernovae from past OB stars produce soft X-rays filling bubbles 50–100 pc in size with  $L_x \sim 10^{35-36}$  ergs/s (Chu & Mac Low 1990).

Figure 10 (left) shows the smoothed ACIS-I image from our original 23-ksec observation of 30 Dor, described in Townsley et al. (2006a,b). Using super-resolution techniques, we find  $\sim 100$  point sources in R136, but clearly the dominant X-ray structures in 30 Dor remain the plasma-filled superbubbles. We constructed maps of the diffuse X-ray emission in those superbubbles, showing variations in plasma temperature ( $T = 3-9$  million degrees), absorption ( $N_H = 1-6 \times 10^{21}$  cm $^{-2}$ ), and absorption-corrected X-ray surface brightness ( $S_{x,corr} = 3-126 \times 10^{31}$  ergs s $^{-1}$  pc $^{-2}$ ). Some new X-ray concentrations  $\simeq 30''$  (7 pc) in extent are spatially associated with high-velocity optical emission line clouds (Chu & Kennicutt 1994). Figure 10 (right) shows the original short ACIS-I observation combined with a new 90-ksec dataset obtained in January 2006. As expected, more point sources are resolved in the longer observation. Smaller-scale diffuse structures are also emerging, likely tracing more subtle shock features across the complex. No obvious hard diffuse emission from a cluster wind in R136 is seen, even in this longer observation.

Figure 11 shows the deeper ACIS image in context with visual and IR data. The center panel shows the recently released H $\alpha$  image from the Magellanic Cloud Emis-

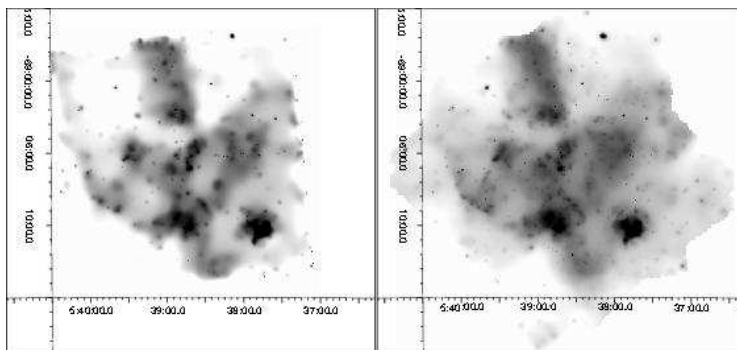


FIGURE 10. *Chandra*/ACIS-I soft-band images of 30 Doradus. **Left:** The original 23-ksec observation. **Right:** New data combined with the original observation, making a  $\sim 110$  ksec image.

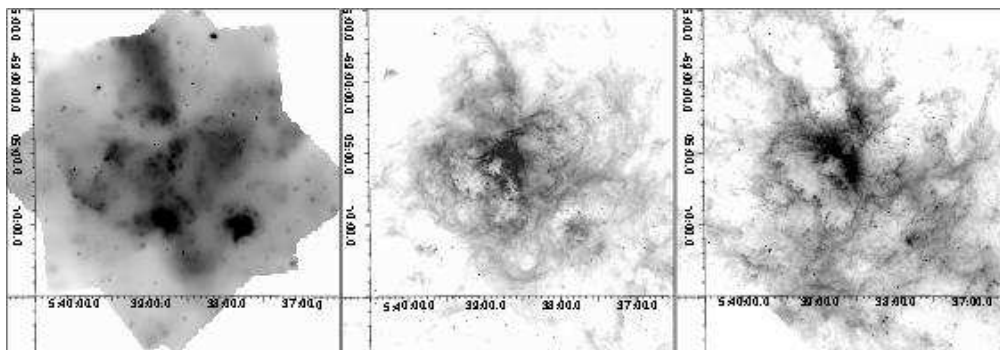


FIGURE 11. 30 Doradus across the spectrum. **Left:** The new soft-band ACIS image. **Center:** An  $H\alpha$  image from MCELS. **Right:** The *Spitzer*  $8\mu\text{m}$  image.

sion Line Survey (MCELS, C. Smith et al. 2000), while the right panel shows the  $8\mu\text{m}$  *Spitzer*/IRAC image (*Spitzer* press release by B. Brandl, 2004). The MCELS and *Spitzer* data gives new insight into the diffuse X-ray structures: the hot superbubbles fill the interiors of ionization fronts outlined by  $H\alpha$  emission, which in turn are outlined by shells of warm dust; the X-ray confinement and morphology are fully appreciated only when anchored by these multiwavelength data.

Our spectral analysis of the superbubbles seen in the early ACIS data revealed a range of absorptions, plasma temperatures, and abundance variations. This short observation limits our ability to study diffuse structures at small scales; in order to get enough counts to do good spectral fitting, we must average over many tens of parsecs. We suspect that we are thus averaging over many distinct plasma components, with different pressures, temperatures, absorbing columns, and possibly even different abundances. The new observation will allow us to refine our spectral fitting and to make higher-resolution maps of the physical parameters that govern 30 Dor’s diffuse X-ray emission. We will also be able to study more completely the massive stars in R136 and throughout the complex.

## 7. Summary

High-resolution X-ray studies of MSFRs reveal magnetically-active pre-MS stars, massive star microshocks, and colliding-wind binaries. *Chandra* provides a disk-unbiased stellar sample for IR study. Diffuse X-ray emission is also seen, caused by O star winds interacting with themselves and with the surrounding media. Supernovae occurring in

the cavities blown by OB clusters produce brighter soft X-rays, dominating the X-ray emission in large multi-cluster and multi-generation star-forming complexes.

Several *Chandra* discoveries are noted in this short overview. For all regions, early O stars often show anomalously hard spectra, perhaps indicating close binarity. For individual regions, discoveries include:

- M17: First clear detection of an X-ray outflow.
- NGC 3576: Bipolar bubble seen in *MSX* data is likely the wind-blown bubble from an embedded OB cluster; this field shows the second clear example of X-ray outflowing gas; hard X-rays reveal cluster members not seen in the IR – these are likely the missing ionizing massive stars.
- W3: W3 Main is huge compared to other W3 young clusters; the W3 Main IRS5 and W3(OH) massive protostars are very hard X-ray sources; W3 North is missing its cluster.
- Tr14: Some early O stars are likely binary or magnetically active, some are not; soft diffuse emission appears between Tr14 and Tr16, while separate, unabsorbed soft diffuse emission located far from massive stars may indicate a cavity supernova remnant inside the Carina complex’s young superbubble.
- 30 Dor: More spatial structure and point sources emerge in the longer observation; no clear sign of hard X-rays from a cluster wind in R136 are seen.

I am most indebted to my colleagues Patrick Broos for data analysis and figure production, Eric Feigelson for ideas and interpretation, and Gordon Garmire, the ACIS PI, for using part of his *Chandra* guaranteed time on the MSFR project. I thank Barbara Whitney and Ed Churchwell for supplying the GLIMPSE image of M17, You-Hua Chu for the MCELS image of 30 Dor, and Bernhard Brandl for the IRAC image of 30 Dor. Support for this work was provided by NASA through contract NAS8-38252 and *Chandra* Awards GO4-5006X, GO4-5007X, GO5-6080X, GO5-6143X, and SV4-74018 issued by the Chandra X-ray Observatory Center, operated by the Smithsonian Astrophysical Observatory for and on behalf of NASA under contract NAS8-03060.

#### REFERENCES

- ARNAUD, K. A. 1996 XSPEC: The First Ten Years. In *Astronomical Data Analysis Software and Systems V* (ed. G. Jacoby & J. Barnes), ASP Conf. Ser. **101**, 17
- BROOKS, K. J., STOREY, J. W. V., & WHITEOAK, J. B. 2001 H110 $\alpha$  recombination-line emission and 4.8-GHz continuum emission in the Carina nebula. *MNRAS*, **327**, 46
- BROOS, P. S., GETMAN, K. V., TOWNSLEY, L. K., FEIGELSON, E. D., WANG, J., GARMIRE, G. P., JIANG, Z., & TSUBOI, Y. 2006 The Young Stellar Population in M17 Revealed by Chandra. *ApJ*, submitted
- CANTÓ, J., RAGA, A. C., & RODRÍGUEZ, L. F. 2000 The Hot, Diffuse Gas in a Dense Cluster of Massive Stars. *ApJ*, **536**, 896
- CARPENTER, J. M., HEYER, M. H., & SNELL, R. L. 2000 Embedded Stellar Clusters in the W3/W4/W5 Molecular Cloud Complex. *ApJS*, **130**, 381
- CHU, Y. & MAC LOW, M. 1990 X-rays from superbubbles in the Large Magellanic Cloud. *ApJ*, **365**, 510
- CHU, Y.-H., & KENNICUTT, R. C., JR. 1994 Kinematic structure of the 30 Doradus giant H II region. *ApJ*, **425**, 720
- DE PREE, C. G., NYSEWANDER, M. C., & GOSS, W. M. 1999 NGC 3576 and NGC 3603: Two Luminous Southern H II Regions Observed at High Resolution with the Australia Telescope Compact Array. *AJ*, **117**, 2902
- DE WIT, W. J., TESTI, L., PALLA, F., & ZINNECKER, H. 2005 The origin of massive O-type field stars: II. Field O stars as runaways. *A&A*, **437**, 247
- DELGADO, A. J., GONZALEZ-MARTIN, O., ALFARO, E. J., & YUN, J. L. 2006 Multiwavelength analysis of the young open cluster NGC 2362. *ApJ*, submitted (astro-ph/0602487)

- EZOE, Y., KOKUBUN, M., MAKISHIMA, K., SEKIMOTO, Y., & MATSUZAKI, K. 2006 Investigation of Diffuse Hard X-Ray Emission from the Massive Star-forming Region NGC 6334. *ApJ*, **638**, 860
- FEIGELSON, E., TOWNSLEY, L., GUDEL, M., & STASSUN, K. 2006 X-ray Properties of Young Stars and Stellar Clusters. To appear in *Protostars & Planets V* (ed. B. Reipurth, D. Jewitt, & K. Keil), Univ. Arizona Press (astro-ph/0602603)
- FIGUERÉDO, E., BLUM, R. D., DAMINELI, A., & CONTI, P. S. 2002 The Stellar Content of Obscured Galactic Giant H II Regions. IV. NGC 3576. *AJ*, **124**, 2739
- FLACCOMIO, E., MICELA, G., & SCIORTINO, S. 2006 ACIS-I observations of NGC2264. Membership and X-ray properties of PMS stars. *A&A*, accepted (astro-ph/0604243)
- FRANCIOSINI, E., PALLAVICINI, R., & SANZ-FORCADA, J. 2006 XMM-Newton observations of the  $\sigma$  Ori cluster. II. Spatial and spectral analysis of the full EPIC field. *A&A*, **446**, 501
- GAGNÉ, M., OKSALA, M. E., COHEN, D. H., TONNESEN, S. K., UD-DOULA, A., OWOCKI, S. P., TOWNSEND, R. H. D., & MACFARLANE, J. J. 2005 Chandra HETGS Multiphase Spectroscopy of the Young Magnetic O Star  $\theta^1$  Orionis C. *ApJ*, **628**, 986
- GETMAN, K. V., FEIGELSON, E. D., TOWNSLEY, L., BROOS, P., GARMIRE, G., & TSUJIMOTO, M. 2006 Chandra Study of the Cepheus B Star-forming Region: Stellar Populations and the Initial Mass Function. *ApJS*, **163**, 306
- HACHISUKA, K., ET AL. 2006 Water Maser Motions in W3(OH) and a Determination of Its Distance. *ApJ*, **645**, 337
- HANSON, M. M., HOWARTH, I. D., & CONTI, P. S. 1997 The Young Massive Stellar Objects of M17. *ApJ*, **489**, 698
- HEYER, M. H., & TEREBEY, S. 1998 The Anatomy of the Perseus Spiral Arm: 12CO and IRAS Imaging Observations of the W3-W4-W5 Cloud Complex. *ApJ*, **502**, 265
- HOFNER, P., DELGADO, H., WHITNEY, B., CHURCHWELL, E., & LINZ, H. 2002 X-Ray Detection of the Ionizing Stars in Ultracompact H II Regions. *ApJL*, **579**, L95
- KRAEMER, K. E., SHIPMAN, R. F., PRICE, S. D., MIZUNO, D. R., KUCHAR, T., & CAREY, S. J. 2003 Observations of Star-Forming Regions with the Midcourse Space Experiment. *AJ*, **126**, 1423
- MAERCKER, M., BURTON, M. G., & WRIGHT, C. M. 2006 L-band ( $3.5 \mu\text{m}$ ) IR-excess in massive star formation. II. RCW 57/NGC 3576. *A&A*, **450**, 253
- MASSEY, P., & HUNTER, D. A. 1998 Star Formation in R136: A Cluster of O3 Stars Revealed by Hubble Space Telescope Spectroscopy. *ApJ*, **493**, 180
- MEGEATH, S. T., WILSON, T. L., & CORBIN, M. R. 2005 Hubble Space Telescope NICMOS Imaging of W3 IRS 5: A Trapezium in the Making? *ApJL*, **622**, L141
- MUNO, M. P., LAW, C., CLARK, J. S., DOUGHERTY, S. M., DE GRIJS, R., PORTEGIES ZWART, S., & YUSEF-ZADEH, F. 2006 Diffuse, Non-Thermal X-ray Emission from the Galactic Star Cluster Westerlund 1. *ApJ*, accepted (astro-ph/0606492)
- NIELBOCK, M., CHINI, R., JÜTTE, M., & MANTHEY, E. 2001 High mass Class I sources in M 17. *A&A*, **377**, 273
- OHEY, M. S., WATSON, A. M., KERN, K., & WALTH, G. L. 2005 Hierarchical Triggering of Star Formation by Superbubbles in W3/W4. *AJ*, **129**, 393
- PERSI, P., ROTH, M., TAPIA, M., FERRARI-TONIOLO, M., & MARENZI, A. R. 1994 The young stellar population associated with the HII region NGC 3576. *A&A*, **282**, 474
- RATHBORNE, J. M., BURTON, M. G., BROOKS, K. J., COHEN, M., ASHLEY, M. C. B., & STOREY, J. W. V. 2002 Photodissociation regions and star formation in the Carina nebula. *MNRAS*, **331**, 85
- REBULL, L. M., STAUFFER, J. R., RAMIREZ, S. V., FLACCOMIO, E., SCIORTINO, S., MICELA, G., STROM, S. E., & WOLFF, S. C. 2006 Chandra X-Ray Observations of Young Clusters. III. NGC 2264 and the Orion Flanking Fields. *AJ*, **131**, 2934
- SANA, H., GOSSET, E., RAUW, G., SUNG, H., & VREUX, J. -. 2006 An XMM-Newton view of the young open cluster NGC 6231 – I. The catalogue. *A&A*, accepted (astro-ph/0603783)
- SANCHAWALA, K., CHEN, W.-P., LEE, H.-T., NAKAJIMA, Y., TAMURA, M., BABA, D., SATO, S., & CHU, Y.-H. 2006 X-ray Emitting Young Stars in the Carina Nebula. astro-ph/0603043
- SKINNER, S. L., SIMMONS, A. E., ZHEKOV, S. A., TEODORO, M., DAMINELI, A., & PALLA,

- F. 2006 A Rich Population of X-Ray-emitting Wolf-Rayet Stars in the Galactic Starburst Cluster Westerlund 1. *ApJL*, **639**, L35
- SMITH, C., LEITON, R., & PIZARRO, S. 2000 The UM/CTIO Magellanic Cloud Emission Line Survey (MCELS). In *Stars, Gas and Dust in Galaxies: Exploring the Links* (ed. D. Alloin, K. Olsen, & G. Galaz), ASP Conf. Ser. **221**, 83
- SMITH, N., EGAN, M. P., CAREY, S., PRICE, S. D., MORSE, J. A., & PRICE, P. A. 2000 Large-Scale Structure of the Carina Nebula. *ApJL*, **532**, L145
- SMITH, N. 2006a A census of the Carina Nebula - I. Cumulative energy input from massive stars. *MNRAS*, **367**, 763
- SMITH, N. 2006b The Structure of the Homunculus. I. Shape and Latitude Dependence from H2 and [Fe II] Velocity Maps of  $\eta$  Carinae. *ApJ*, **644**, 1151
- SMITH, R. K., BRICKHOUSE, N. S., LIEDAHL, D. A., & RAYMOND, J. C. 2001 Collisional Plasma Models with APEC/APED: Emission-Line Diagnostics of Hydrogen-like and Helium-like Ions. *ApJL*, **556**, L91
- STASSUN, K. G., VAN DEN BERG, M., FEIGELSON, E., & FLACCOMIO, E. 2006 A Simultaneous Optical and X-ray Variability Study of the Orion Nebula Cluster. I. Incidence of Time-Correlated X-ray/Optical Variations. *ApJ*, accepted (astro-ph/0606079)
- TIEFTRUNK, A. R., GAUME, R. A., CLAUSSEN, M. J., WILSON, T. L., & JOHNSTON, K. J. 1997 The H II/molecular cloud complex W3 revisited: imaging the radio continuum sources using multi-configuration, multi-frequency observations with the VLA. *A&A*, **318**, 931
- TOWNSLEY, L. K., FEIGELSON, E. D., MONTMERLE, T., BROOS, P. S., CHU, Y., & GARMIRE, G. P. 2003 10 MK Gas in M17 and the Rosette Nebula: X-Ray Flows in Galactic H II Regions. *ApJ*, **593**, 874
- TOWNSLEY, L., FEIGELSON, E., MONTMERLE, T., BROOS, P., CHU, Y. -, GARMIRE, G., & GETMAN, K. 2004 Parsec-Scale X-ray Flows in High-Mass Star-Forming Regions. Proc. of *X-ray and Radio Connections* Workshop, Santa Fe, NM, February 2004, astro-ph/0406349
- TOWNSLEY, L. K., BROOS, P. S., FEIGELSON, E. D., & GARMIRE, G. P. 2005 Parsec-scale X-ray flows in high-mass star-forming regions. In *IAU Symp. 227, Massive Star Birth - A Crossroads of Astrophysics* (ed. R. Cesaroni, E. Churchwell, M. Felli, & C. M. Walmsley), p. 297. Cambridge University Press (astro-ph/0506418)
- TOWNSLEY, L. K., BROOS, P. S., FEIGELSON, E. D., BRANDL, B. R., CHU, Y.-H., GARMIRE, G. P., & PAVLOV, G. G. 2006a A *Chandra* ACIS Study of 30 Doradus. I. Superbubbles and Supernova Remnants. *AJ*, **131**, 2140
- TOWNSLEY, L. K., BROOS, P. S., FEIGELSON, E. D., GARMIRE, G. P., & GETMAN, K. V. 2006b A *Chandra* ACIS Study of 30 Doradus. II. X-Ray Point Sources in the Massive Star Cluster R136 and Beyond. *AJ*, **131**, 2164
- TSUJIMOTO, M., TOWNSLEY, L., FEIGELSON, E. D., BROOS, P., GETMAN, K. V., & GARMIRE, G. 2005 Chandra Observations of Galactic HII Regions; NGC 7538 & W49A. *Protostars and Planets V*, 8307
- TSUJIMOTO, M., HOSOKAWA, T., FEIGELSON, E. D., GETMAN, K. V., & BROOS, P. 2006 Hard X-rays from Ultracompact HII Regions in W49A. *ApJ*, accepted
- VÁZQUEZ, R. A., BAUME, G., FEINSTEIN, A., & PRADO, P. 1996 Investigation on the region of the open cluster TR 14. *A&AS*, **116**, 75
- WALBORN, N. R., ET AL. 2002a A New Spectral Classification System for the Earliest O Stars: Definition of Type O2. *AJ*, **123**, 2754
- WALBORN, N. R., DANKS, A. C., VIEIRA, G., & LANDSMAN, W. B. 2002b Space Telescope Imaging Spectrograph Observations of High-Velocity Interstellar Absorption-Line Profiles in the Carina Nebula. *ApJS*, **140**, 407
- WANG, J., TOWNSLEY, L. K., FEIGELSON, E. D., GETMAN, K. V., BROOS, P. S., GARMIRE, G. P., TSUJIMOTO, M. 2006 A Chandra Study of the NGC 6357 Star-forming Complex. *ApJS*, submitted
- WANG, Q. D., DONG, H., & LANG, C. 2006 The Interplay between Star Formation and the Nuclear Environment of our Galaxy: Deep X-ray Observations of the Galactic Center Arches and Quintuplet Clusters. *MNRAS*, accepted (astro-ph/0606282)
- WOLK, S. J., SPITZBART, B. D., BOURKE, T. L., & ALVES, J. 2006 X-ray and IR Point Source Identification and Characteristics in the Embedded, Massive Star-Forming Region RCW 38. *ApJ*, accepted (astro-ph/0605096)